Evaluating Retina Image Fusion Based on Quantitative Approaches

ZHENGMAO YE[1], HUA CAO[2], SITHARAMA IYENGAR[2], HABIB MOHAMADIAN[1]
[1]Southern University, Baton Rouge, LA 70813, USA
zhengmaoye@engr.subr.edu; mohamad@engr.subr.edu
[2]Louisiana State University, Baton Rouge, LA 70803, USA
hcao@csc.lsu.edu; iyengar@csc.lsu.edu

Abstract: - Image registration and fusion are conducted using an automated approach, which applies the automatic adaptation from frame to frame with the threshold parameters. Rather than qualitative approach, quantitative measures have been proposed to evaluate outcomes of retina image fusion. Concepts of the discrete entropy, discrete energy, relative entropy, mutual information, uncertainty coefficient and information redundancy have been introduced. Both the Canny edge detector and control point identification are employed to extract retinal vasculature using the adaptive exploratory algorithms. The shape similarity criteria have been selected for control point matching. The Mutual-Pixel-Count maximization based optimal procedure has also been developed to adjust the control points at the sub-pixel level. Then the global maxima equivalent result has been derived by calculating Mutual-Pixel-Count local maxima. For two cases of image fusion practices, the testing results are evaluated on a basis of information theories where the satisfactory outcomes have been made.

Key-Words: - Image Fusion, Image Registration, Histogram, Discrete Energy, Discrete Entropy, Relative Entropy, Mutual Information, Uncertainty Coefficient, Information Redundancy

1 Introduction

Comparison between the angiogram gray scale and fundus color images is generally required in order to identify dynamic aspects of circulation in practical applications and to evaluate various retinal vascular disorders. The regular methods for medical image registration and fusion are either area-based or feature-based. Mutual Information (MI) is the frequently used optimization measurement in the area-based fusion. Maximization is a major approach for the area-based technique [1-5]. An algorithm for the detection of red lesions in digital color fundus photographs has been proposed. One set of correlation filters at different resolutions is used to select candidates from a wider set of points. The growing segmentation process rejects the points from the prior stage whose size does not fit. Afterwards the shape test is used to remove non-circular areas, the intensity test is used to remove the retina fundus areas and another test is used to remove the points inside the vessels. Evaluation is performed and comparison is made to set accuracy and reliability of the method [5].

We employ the MI concept and then simplify it into Mutual-Pixel-Count (MPC). The MPC measures the overlap pixels of the retinal vasculature. When images are perfectly geometrically aligned, the feature-based fusion method extracts and matches the common structures (features) from two images. It has been proved to be able to receive the higher successful rate at the multi-modality fusion scenario than that of the area-based method. This feature refers to the salient structure, such as the central line of vessels and vessel bifurcation points in the retinal network. Depend on the transformation model, the feature-based method requires a certain number of control points [6-9]. Data mining methods of neural network, rough sets and support vector machine (SVM) have received more and more attentions and have been widely applied to areas of sensing classification. Comparison results are made where each has its advantage and disadvantage. Combination of these theories on sensing applications is an important tendency [10]. The computer aided detection of pulmonary nodules in X-ray CT images has been applied to reduce false positive rate under the high true positive rate conditions. By using the variation feature of shadows in the direction along the body axis, the method selects the actual candidates, instead of all the images, the method discriminates nodules from non-nodules by using orientation feature details of shadow shapes. This selection results in less computational expense [11].

The proposed approach selects a combined method, which employs the feature-based method in image registration and the area-based method in image fusion. For the feature-based registration, the adaptive exploratory algorithm has been used to identify the global direction change pixel at the Canny edges. By locating control points at the global direction change pixel, the local direction changes will be effectively avoided. For the area-based fusion, the MPC has been introduced, which is a new and unique concept in the biomedical image fusion area, especially for the fusion accuracy measurement. The fusion result is assumed to be optimal when the MPC reaches the maximum value. From the information theory, concepts of the discrete entropy, discrete energy, relative entropy, mutual information and uncertainty coefficient as well as information redundancy are introduced to evaluate all the outcomes of image fusion. In this case, both quantitative measures and qualitative observations are used jointly in this research [1-27].

2 Retinal Image Acquisition

Retinal images presented in this paper are taken by a Topcon TRC-50EX fundus camera. The subjects of the retinal images are five Cynomolgus monkeys of 4 to 4.5 years of age and 2.5 to 3 kg body weight with the normal eyes [3]. The experimental monkeys are anesthetized with the intramuscular ketamine, xylazine and intravenous pentobarbital (7-10 mg/kg, 0.6-1 mg/kg and 25-30 mg/kg, respectively). Administration of the anesthetics is repeated alternately every 30 minutes as required to maintain the animal in deep, stage IV anesthesia [3]. Establishing animal models is an essential prerequisite of the development of new therapeutic interventions on human diseases. Monkey species provide appropriate preclinical models that can closely reflect human's physical and physiological characteristics because of the very close phylogenetic relationship to human beings [4].

3 Feature-Based Multi-Modality Registration of Retinal Images Using Adaptive Algorithm

3.1 Image Binarization via Discriminant Analysis

Prior to fusion, image pairs need to be registered pixel-by-pixel through a mapping function. In this new registration algorithm, we firstly binarize the reference and input images. The angiogram grayscale image is the reference image, and the fundus color image is the input image. The global adaptive threshold developed by Otsu [6][7] is used to convert the gray level colors to merely black and white. The output binary image has values of 0 (black) for all pixels with the original luminance and intensity less than Otsu's threshold and 1 (white) for all other pixels. The threshold is one normalized intensity value that lies in the range [0, 1].

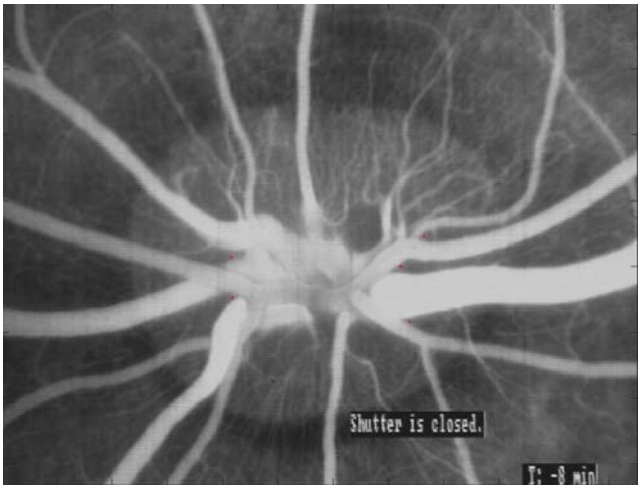

Fig. 1 Angiogram Grayscale Image (Otsu Threshold)

Fig. 2 Angiogram Binary Image (Otsu Threshold)

The Otsu's method chooses the optimal threshold to minimize the intra-class variance of the black and white pixels and to maximize between-class variance in a grayscale image. The algorithm calculates the statistics of the image itself to set the threshold and use the histogram to choose its value at some percentile as a reference value of the region strength. Therefore, Otsu's method is non-parametric and non-supervised. When binarizing a color image, it is converted into 8-bit gray scale prior to the binary image. 0.5236 for red,

0.1232 for green and 0.3256 for blue are the default weight parameters. From this method, we extract the blue color as an example when converting to gray scale image because the blue intensity histogram is the closest one to the normal distribution and vessels on the retinal images contain stronger average blue color information than those of red and green or any other RGB combination. Using the Otsu threshold, the source angiogram image and binary angiogram image are shown in Figs. 1-2, and the source Fundus image and binary Fundus image are shown in Figs. 3-4.

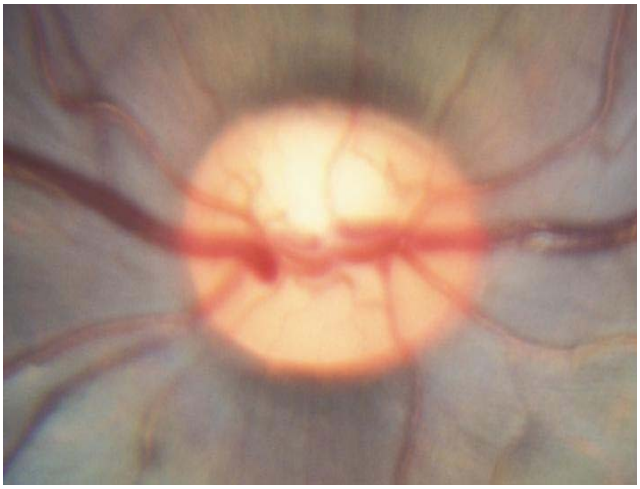

Fig. 3 Fundus Color Image (Otsu Threshold)

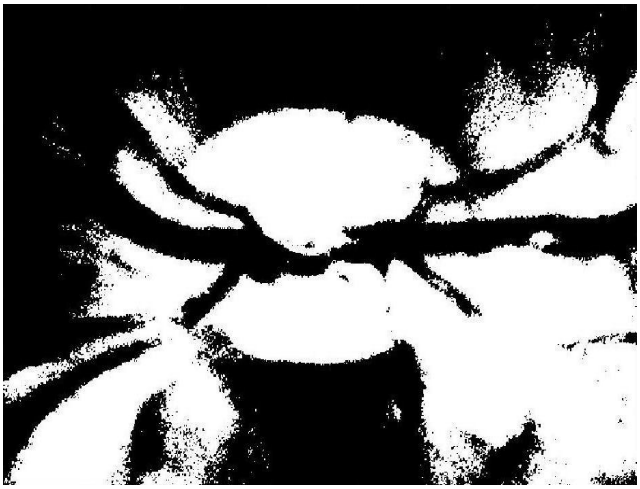

Fig. 4 Fundus Binary Image (Otsu Threshold)

3.2 Extract Vasculature via Canny Edge Detector

A digital curve display is represented by an integer sequence based on the position of the current edge pixel to the eight neighbors at the 2D spatial domain: Ni {1, 2, 3, 4, 5, 6, 7, 8}, representing the evenly distributed angles. The Canny edge detector detects the edges at zero-crossings of the second directional derivative of the image. The zero-crossings of Canny's method correspond to the first directional-derivative's maxima and minima in the direction of the gradient. Each pixel's edge gradient is computed and compared with the gradients of its neighbors along the gradient direction. If the gradient at $P_{x,y}$ is greater than both the $P_{x+1,y+1}$ and $P_{x-1,y-1}$, then the $P_{x,y}$ will be identified as the maxima simply.

3.3 Control Points Adaptive Selection

We select the control points at the vessel bifurcations on the Canny edge. The vessel tracking is efficiently performed in the adaptive exploratory algorithm without traveling at every pixel. The vasculature is traced by locating an initial point and exploiting the local neighbors [5]. Firstly the entire image is split into two equal size bifurcation blocks of West and East. Considering retinal images, good control points always come out of the east or west side of the optic disk, rather than the north or south side. From the west block's Northwest corner, read the edge pixels from west to east and from north to south. Mark the current direction as the "East" whenever the edge pixels are heading toward East, Southeast, or Northeast. Increase the step count once when the pixel is moving toward "East", while the straight North or straight south does not count for steps.

If the direction starts to change, i.e. changes from east to west, the step count needs to be compared with ROLLBACK threshold step. If smaller, roll back the most recent change of step count; otherwise, keep the last step direction and reset the step count. The direction-changing pixel is a possible control point to be determined later. Repeat this sequence and mark the most recent possible control point as a true control point when the step count is equal to the threshold MAXSTEP and the previous step count is equal or greater than the MAXSTEP as well. At the east block, read the Canny edge pixels from east to west. The rest procedures are the same except the direction reading the edge pixels is from East to West, and the direction change sign is from westward to eastward.

The control point selection for source images of Monkey 1 are shown in Figs. 5-6, and the control point selection for source images of Monkey 2 are shown in Figs. 7-8, where cases of both angiogram image and Fundus image have been considered.

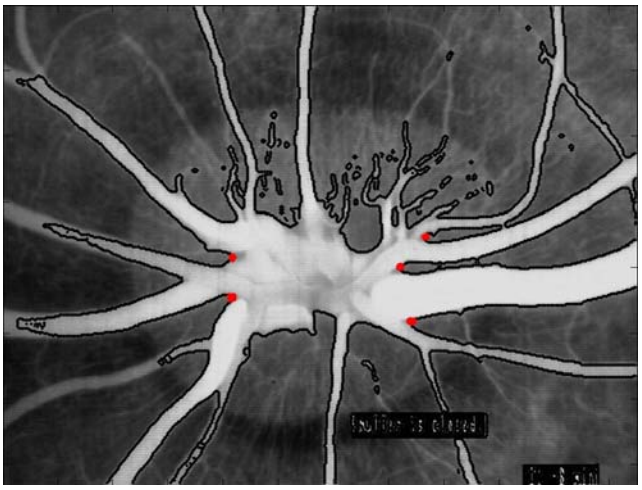

Fig. 5 IVFA Image Control Point Selection (Case 1)

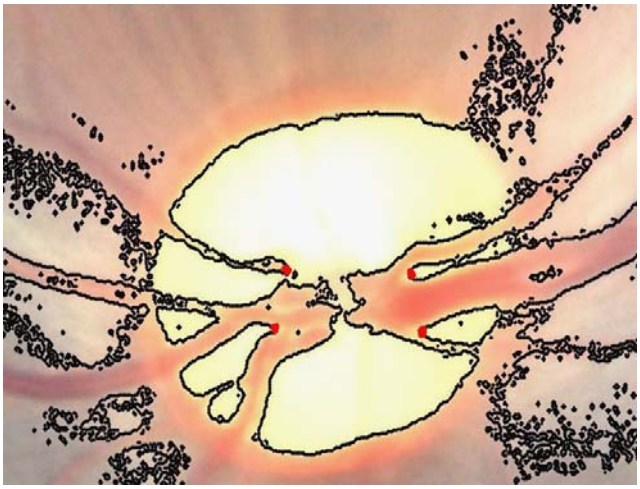

Fig. 6 Fundus Image Control Point Selection (Case 1)

Fig. 7 IVFA Image Control Point Selection (Case 2)

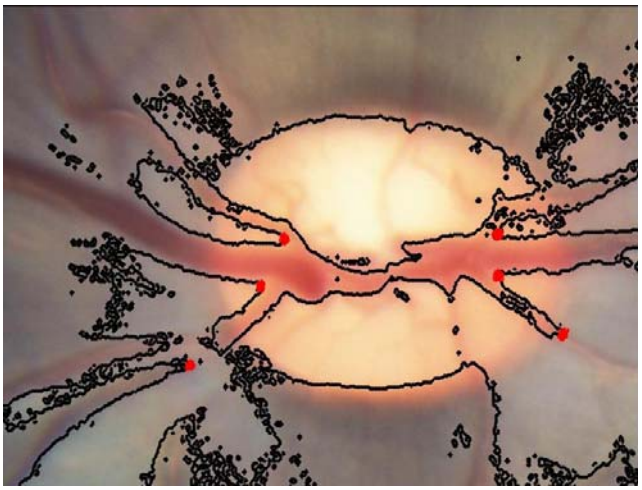

Fig. 8 Fundus Image Control Point Selection (Case 2)

3.4 Control Point Pair Matching Via Similarity

The 2D affine transformation model requires three pairs of control points $\{(x_i, y_i), (u_i, v_i)\}$ (i = 1, 2, 3). The first element of each pair is from the reference image and the second element is from the input image. Firstly, the image having less number of control points is taken as the grouping base. Suppose the image one has n control points, and the image two has m control points, and m < n, then m will be the group number for which how many groups of the control points are available. Secondly, all control points are combined in the image one with each control point in the image two, and thus all m by n control point pairs can be obtained totally. Now the distance |d| can be calculated between each control point pair within each group. Thirdly, inside each group, the pair with minimum |d| is chosen. The assumption we use the distance as the measurement of the control point pairs is based on the fact that two images do not have significant rotation, shearing or translation, and thus the same features on each image are close to each other. If there are two or more control points in one image matching the same control point in the other image, the true match will always have smaller |d| than the false match. Finally, the three smallest distance control point pairs are selected as the final (x, y) and (u, v) pairs for the transformation model of the retina images.

4 Optimization Fusion Based on Mutual Pixel Count Maximization

A successful fusion is one with a good superposition of retinal blood vessels. The combined image created from the control points selected in the previous

registration step does not meet such criteria. An optimization procedure is needed to adjust these control points in order to achieve an optimal result. A new automated optimization iteration algorithm has been developed based on the Mutual-Pixel-Count maximization. A refinement of the solution is obtained at the end of each loop, and finally a satisfying fusion image is generated at the end of the iteration.

4.1 Mutual Pixel Count (MPC)

The MPC measures the retinal vasculature overlap for corresponding pixels in both source images. When the vasculature pixel (black) transforms (u, v) coordinates on the input image are corresponding to a vasculature pixel's (x, y) coordinates on the reference image, the MPC is incremented by one. MPC is assumed to be maximal if the image pair is geometrically aligned by the transformation.

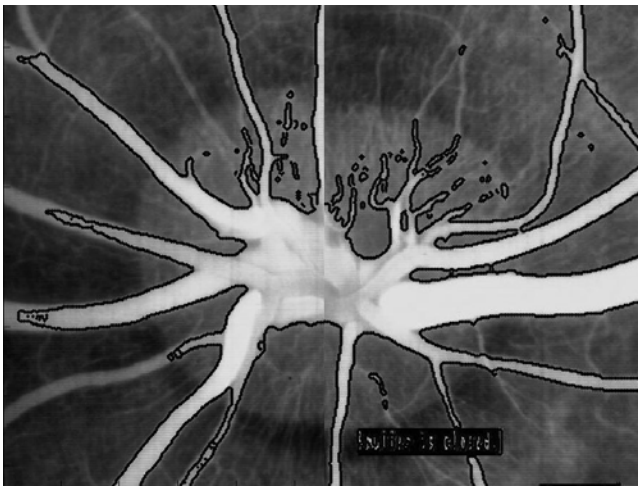

Fig. 9 Source IVFA Image (Case 1)

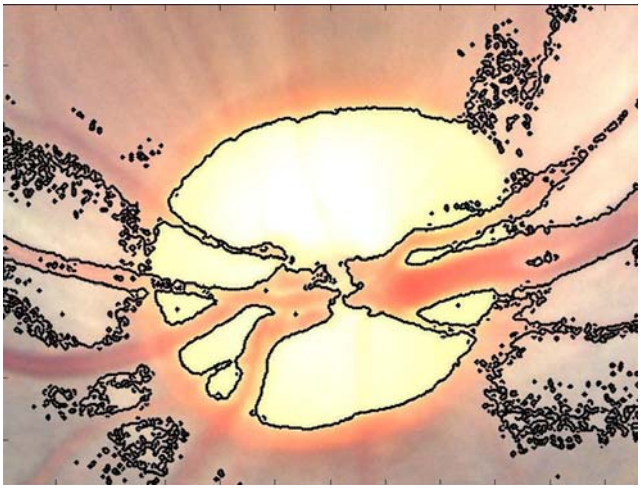

Fig. 10 Source IVFA Image (Case 1)

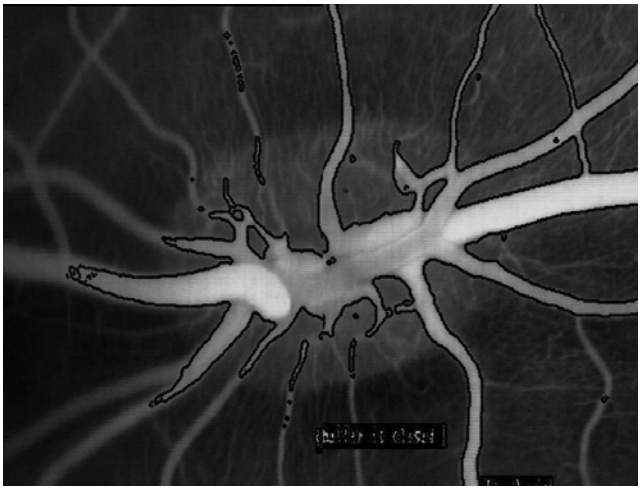

Fig. 11 Source IVFA Image (Case 2)

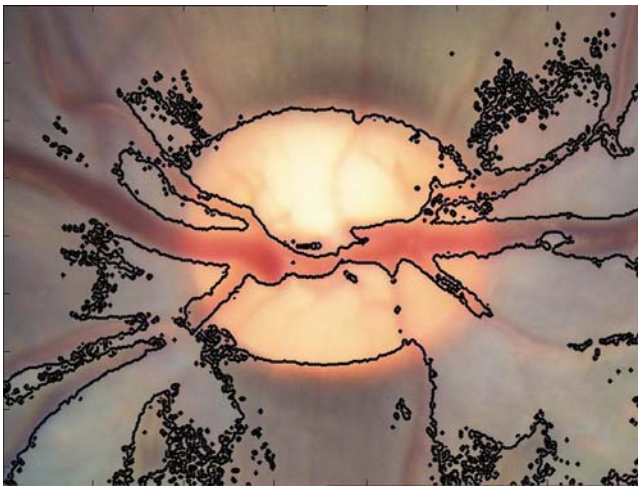

Fig. 12 Source IVFA Image (Case 2)

Using this approach, source angiogram and Fundus images of both the Monkey 1 and Monkey 2 have been selected. These source images are shown in Figs. 9-12, respectively.

4.2 Global Maxima v.s. Local Maxima

To achieve optimization, global optimization scheme is desirable to achieve global maxima, but with the tradeoff on expensive computation cost. In practice, a local optimization schema is usually employed to reduce computation cost. However, local optimization can be attracted to local maxima. Thus, a new local maxima scheme is developed to achieve a global maxima equivalent result at an efficient computation cost. The entire retinal vasculature is split into three regions, i.e. west region, middle region (optic nerve head), and east region.

Only two regions out of three are selected for MPC calculation. The east region and west region are the preferred ones. The middle region is the backup in case that either of the former regions is not qualified. If the black area of the west region from the binary image is greater than the threshold, it will not be selected. By calculating partial retinal vasculature, we are able to obtain an optimal result by achieving a maximal MPC that is very close to the global maxima. If the side region reaches over a certain threshold percentage of black area, the retinal vessels cannot be well extracted among the overwhelming black pixels.

4.3 Optimization Iteration

Our optimization algorithm finds an optimal similarity measure by refining transformation parameters in an ordered way. During the iteration, control points of the reference image are fixed and that of the input image are subject to adjustment.

Increase control point's x coordinate by a step size s initially. If the MPC is increased due to movement, keep increasing by the step size s until MPC stops increasing. Repeat this sequence for y coordinate as well. Secondly decrease control point's x coordinate and y coordinate by a step size s until MPC increasing. Repeat this sequence for all other control points until MPC stops increasing. A maximum allowable loop number is set to avoid redundant computation for mismatched control points, which leads to the fusion failure. Convergence criteria are used to determine when the iteration is finished.

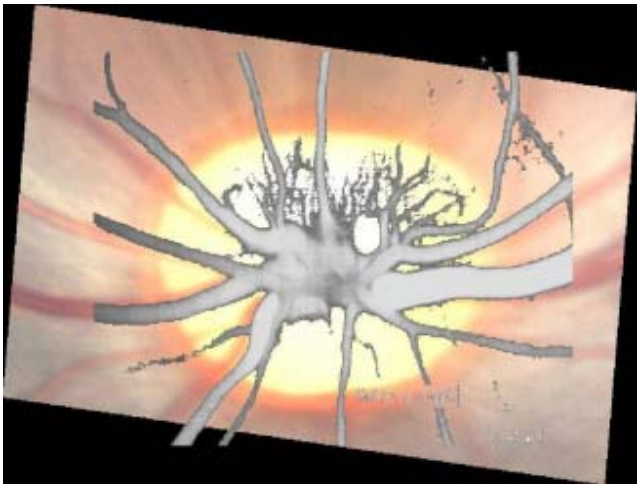

Fig. 13 Fusion Images of Monkey Case 1

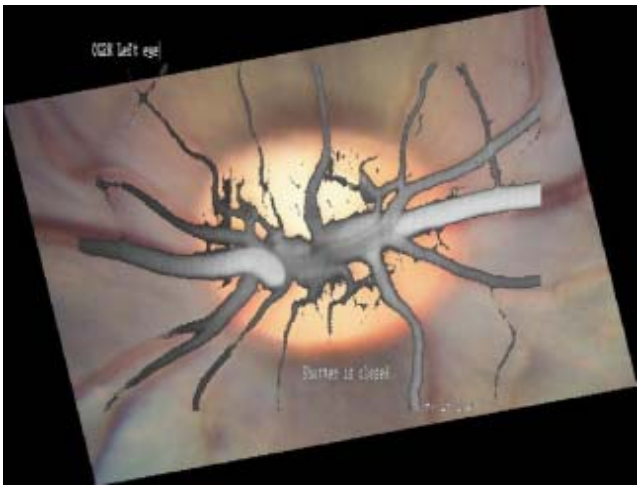

Fig. 14 Fusion Images of Monkey Case 2

4.4 Parameters Extraction

Once there are three pairs control points' coordinates available, it is possible to apply them to the 2D affine model and then solve the Gaussian matrix to get the parameters P {a1, a2, a3, a4, b1, b2}.

$$\begin{bmatrix} u_1 \\ v_1 \\ u_2 \\ v_2 \\ u_3 \\ v_3 \end{bmatrix} = \begin{bmatrix} x_1 & y_1 & 1 & 0 & 0 & 0 \\ 0 & 0 & 0 & x_1 & y_1 & 1 \\ x_2 & y_2 & 1 & 0 & 0 & 0 \\ 0 & 0 & 0 & x_2 & y_2 & 1 \\ x_3 & y_3 & 1 & 0 & 0 & 0 \\ 0 & 0 & 0 & x_3 & y_3 & 1 \end{bmatrix} \begin{bmatrix} a_1 \\ a_2 \\ b_1 \\ a_3 \\ a_4 \\ b_2 \end{bmatrix} \quad (1)$$

5 Histogram and Probability Functions

An automatic approach for multi-modality retinal image registration has been developed using the feature-based method. Image binarization is the first step, which is to provide the input data for the Canny edge detector. The selected Otsu method chooses the optimal threshold to minimize the intra-class variance of the black and white pixels, and to maximize the between-class variance in the gray scale image, which is a nonparametric and unsupervised method. The discrete image with N*M pixels is considered, with retinal vessels (objects) in one class and the optic disk (background) in another class. Occurrence of color component level is described as co-occurrence matrix of relative frequencies. The occurrence probability function is then estimated from its histogram, which is formulated as (2):

$$p(k)=\frac{h(k)}{\sum h(k)} \quad (2)$$

where p(k) is the probability distribution function and h(k) is the histogram function.

6 Discrete Entropy in Image Fusion

The discrete entropy is a measure of information content, which is interpreted as the average uncertainty of the information source. The discrete entropy is the summation of products of the probability of the outcome multiplied by the logarithm of the inverse of probability of the outcome, taking into considerations of all possible outcomes {1, 2, …, n} as the color component level in the event $\{x_1, x_2, \ldots, x_n\}$, where p(i) is the probability at the level i, which contains all the histogram counts. The discrete entropy H(x) is formulated as (3) and the corresponding results are shown in Table 1.

$$H(x)=\sum_{i=1}^{k} p(i)\log_2 \frac{1}{p(i)} = -\sum_{i=1}^{k} p(i)\log_2 p(i) \qquad (3)$$

Table 1 Entropy of Image Fusion for Monkey 1 and Monkey 2

Global Entropy	Image A	Image B	Fusion
Monkey 1	7.3842	6.9680	6.5326
Monkey 2	6.7391	7.3238	6.1550

7 Discrete Energy in Image Fusion

The discrete energy measure indicates how the color elements are distributed. Its formulation is shown in (4), where E(x) represents the discrete energy with 256 bins and p(i) refers to the probability distribution functions at different color levels, which contains the histogram counts. For any constant value of the color component level, the energy measure reaches its maximum value of 1. The larger energy corresponds to lower color component level numbers and the smaller one corresponds to higher color component level numbers. The discrete energy of the source images and fusion images are shown in Table 2.

$$E(x)=\sum_{i=1}^{k} p(i)^2 \qquad (4)$$

Table 2 Energy of Monkey 1 and Monkey 2

Energy	Image A	Image B	Fusion
Monkey 1	0.0076	0.0098	0.0359
Monkey 2	0.0133	0.0077	0.0713

8 Relative Entropy in Image Fusion

Suppose two discrete probability distributions of the processing images have the probability functions of p(i) and q(i). The relative entropy of p with respect to q is then defined as the summation of all possible states of the system, which is formulated as (5). The relative entropy of the source image and fusion image is shown in Table 3.

$$d=\sum_{i=1}^{k} p(i)\log_2 \frac{p(i)}{q(i)} \qquad (5)$$

Table 3 Relative Entropy in Image Processing

Relative Entropy	Fusion v.s. Image A	Fusion v.s. Image B
Monkey 1	2.5688	1.1505
Monkey 2	2.5927	1.1806

9 Mutual Information in Image Fusion

Another concept of the mutual information I(X; Y) can be applied also, which is used to describe how much information one variable tells about the other variable. The relationship is formulated as (6).

$$\begin{aligned} I(X;Y) &= \sum_{X,Y} p_{XY}(X, Y)\log_2 \frac{p_{XY}(X, Y)}{p_X(X)p_Y(Y)} \\ &= -\sum_{X} p_X(X)\log_2 p_X(X) + \sum_{X, Y} p_{XY}(X, Y)\log_2 \frac{p_{XY}(X, Y)}{p_Y(Y)} \\ &= H(X) - H(X|Y) \end{aligned} \qquad (6)$$

where H(X) and H(X|Y) are values of the entropy and conditional entropy; p_{XY} is the joint probability density function; p_X and p_Y are marginal probability density functions. It can be explained as information that Y can tell about X is the reduction in uncertainty of X due to the existence of Y. It can also be regarded as the relative entropy between joint distribution and product distribution. Results of mutual information between the original and fused images are shown in Table 4.

Table 4 Mutual Information Between Images

Mutual Information	Fusion and Image A	Fusion and Image B
Monkey 1	0.8517	0.4354
Monkey 2	0.5841	1.1687

10 Normalized Mutual Information

The normalized mutual information is the measure covering content from individual discrete entropies and mutual information. It is formulated as (7).

$$N\_MI=\frac{I(X;Y)}{\sqrt{H(X)H(Y)}} \quad (7)$$

where I(X, Y) is the mutual information; H(x) and H(y) are the discrete entropies. The results are shown in Table 5.

Table 5 Normalized MI Between Images

Normalized MI	Fusion Image 1	Normalized MI	Fusion Image 2
Monkey 1	0.1226	Monkey 1	0.0645
Monkey 2	0.0907	Monkey 2	0.1741

Another pointwise mutual information is also the measure of association in the information theory. The pointwise mutual information of outcomes x and y belonging to discrete random variables quantifies the inconsistency between the probability of coincidence given joint distributions versus the probability of the coincidence given individual distributions. It has been formulated as (8).

$$P\_MI(x, y)=\log\frac{p(x; y)}{p(x)p(y)} \quad (8)$$

where p(x) and p(y) are the probability distribution functions, p(x, y) is the joint probability function. This measure takes a similar role as the mutual information and normalized mutual information.

11 Uncertainty Coefficient

An uncertainty coefficient presents the uncertainty in the dependent variable. It is based on the entropy principle to ascertain the uncertainty in the dependent variable and calculate the proportion of uncertainty. It ranges from 0 to 1, which indicates the normalized variants of the mutual information, where 0 refers to no reduction in uncertainty of the dependent variable and 1 refers to the complete elimination of uncertainty. An uncertainty coefficient is a non-symmetric function which is defined as (9) and the corresponding results for the money retina images are shown in Table 6.

$$C_{XY} = I(X;Y) / H(Y);\ C_{YX} = I(X;Y) / H(Y) \quad (9)$$

Table 6 Uncertainty Coefficients in Image Processing

Uncertainty Coefficient	Fusion - Image A C_{XY}	Fusion - Image A C_{YX}	Fusion - Image B C_{XY}	Fusion - Image B C_{YX}
Monkey 1	0.0798	0.0867	0.1596	0.1734
Monkey 2	0.1222	0.1153	0.0625	0.0590

12 Image Fusion Redundancy

The symmetric information measure can be introduced to indicate redundancy in image fusion, which reaches the minima of zero when all variables are independent. It is formulated as (10):

$$R=\frac{I(X;Y)}{H(X)+H(Y)} \quad (10)$$

where H(X) and H(Y) are entropies of two raw images and I(X, Y) is the mutual information. For cases of monkeys 1 and 2, the information redundancy between the fused image and raw images are shown in Table 7.

Table 7 Information Redundancy of Image Fusion

Information Redundancy	Fusion and Image A	Fusion and Image B
Monkey 1	0.0593	0.0303
Monkey 2	0.0415	0.0831

13 Conclusion

An automatic approach for multi-modality retinal image registration has been proposed and developed using the feature-based method, which can also be evaluated in both quantitative and qualitative methods. This approach is robust to handle multi-sensor retinal image registration as long as the input image does not involve the significant rotation or translation when compared with the reference image. The mismatch occurs if there is the huge rotation or translation of the input images, which some regular feature-based approaches have difficulties in dealing with. The suitable solution is to implement the area-based registration method to align the image beforehand. Then the feature-based multi-modality registration algorithm proposed will serve as the fundamental step for the hybrid area-based and feature-based systems, which can be easily applied to a wide variety of medical examples in some practical implementations.

To investigate the details of some complex processes quantitatively, the information theory has successfully been applied. The concepts of the discrete entropy, discrete energy, relative entropy, mutual information, uncertainty coefficient and information redundancy have been employed as measures to evaluate image registration and image fusion.

References:

[1] F. Maes, A. Collignon, et al, "Multimodality Image Registration by Maximization of Mutual Information", *IEEE Transactions on Medical Imaging*, 1997, V 16, N2, pp. 187-198.

[2] Z. Ye, H. Cao, S. Iyengar and H. Mohamadian, "Medical and Biometric System Identification for Pattern Recognition and Data Fusion with Quantitative Measuring", Chapter Six, *Systems Engineering Approach to Medical Automation*, Artech House Publishers, 2008, pp. 91-112

[3] Z. Ye, "Artificial Intelligence Approach for Biomedical Sample Characterization Using Raman Spectroscopy", *IEEE Transactions on Automation Science and Engineering*, Volume 2, Issue 1, pp. 67-73, ITASC7, ISSN 1545-5955, January, 2005

[4] J. Beach, J. Ning and B. Khoobehi, "Oxygen Saturation in Optic Nerve Head Structures by Hyperspectral Image Analysis", *Current Eye Research*, V32, 2007, pp. 161-170

[5] C. Marino, E. Ares, M. Penedo, et al, "Automated Three Stage Red Lesions Detection In Digital Color Fundus Images", *WSEAS Transactions on Computers*, Issue 4, Vol 7, April 2008, pp.207-15

[6] N. Otsu, "A Threshold Selection Method from Gray-Level Histograms", *IEEE Transactions on Systems, Man, & Cybernetics*, V9, P 62-66, 1979

[7] P. Sahoo, A. Farag, Y. Yeap, "Threshold Selection Based on Histogram Modeling", *IEEE Transactions on Systems, Man and Cybernetics*, V1, Oct, 1992, pp. 351 – 356

[8] J. Canny, " A Computational Approach To Edge Detection", *IEEE Transactions on Pattern Analysis and Machine Intelligence*, V8, November 1986, pp. 679-698

[9] W. Green, "Canny Edge Detector", Department of Mechanical Engineering, Drexel University, Philadelphia, PA 19104, 2002

[10] H. Xiao and X. Zhang, "Comparison Studies on Classification for Remote Sensing Image Based on Data Mining Method", *WSEAS Transactions on Computers*, Issue 5, Vol 7, May 2008, pp.552-8

[11] N. Homma, K. Takei, "Combinatorial Effect of Various Features Extraction on Computer Aided Detection of Pulmonary Nodules in X-ray CT Images", *WSEAS Transactions on Information Science and Applications*, Issue 7, Volume 5, July 2008, pp. 1127-1136

[12] G. Matsopoulos, N. Mouravliansky and K. Delibasis, "Automatic Retinal Image Registration Scheme Using Global Optimization Techniques", *IEEE Transactions on Information Technology in Biomedicine*, V3, March 1999, pp. 47 - 60

[13] F. Laliberte, L. Gagnon, "Registration and fusion of retinal images - An evaluation study", *IEEE Transactions on Medical Imaging*, 2003, V22, N5, pp. 661-673

[14] H. Cao, "A Novel Automated Approach of Multi-modality Retinal Image Registration and Fusion", Ph.D. Dissertation, Louisiana State University, Baton Rouge, LA, 2008

[15] T. Cover, J. Thomas, *Elements of Information Theory*, 2nd Edition, New York: Wiley, 2005

[16] D. MacKay, *Information Theory, Inference and Learning Algorithms*, University of Cambridge Press, 2005

[17] Z. Ye, Y. Ye, H. Yin and H. Mohamadian, "Integration of Wavelet Fusion and Adaptive Contrast Stretching for Object Recognition with Quantitative Assessment", *International Journal on Graphics, Vision and Image Processing*, ISSN 1687-398X, V(8), Jan 2009, pp. 33-42

[18] Z. Ye, H. Mohamadian and Y. Ye, "Gray Level Image Processing Using Contrast Enhancement and Watershed Segmentation with Quantitative Evaluation", 2008 IEEE International Conference on Content-Based Multimedia Indexing (CBMI 2008), pp. 470-5, June 18-20, 2008, London, UK

[19] Z. Ye, H. Mohamadian and Y. Ye, "Independent Component Analysis for Spatial Object Recognition with Applications of Information Theory Synthesis", 2008 IEEE World Congress on Computational Intelligence (WCCI 2008), IEEE International Joint Conference on Neural Networks (IJCNN 2008), pp. 3640-5, Hong Kong, June 1-6, 2008

[20] Z. Ye, H. Mohamadian and Y. Ye, "Sensing Data Discrete Wavelet Fusion for Pattern Recognition with Qualitative and Quantitative Measuring", 2008 IEEE World Congress on Computational Intelligence (WCCI 2008), 2008 IEEE International Joint Conference on Neural Networks (IJCNN 2008), pp. 3646-51, Hong Kong, June 1-6, 2008

[21] Z. Ye, H. Mohamadian, S. Pang and S. Iyengar, "Contrast Enhancement and Cluster Segmentation of Gray Level Images with Quantitative Information Evaluation", *WSEAS Transactions on Information Science and Applications*, Volume 5, Issue 2, pp. 181-188, February, 2008

[22] Z. Ye, H. Mohamadian and Y. Ye, "Practical Approaches on Enhancement and Segmentation of Trimulus Color Image with Information Theory Based Quantitative Measuring", *WSEAS Transactions on Signal Processing*, Vol 4, Issue 1, pp. 12-20, January, 2008

[23] Z. Ye, H. Mohamadian and Y. Ye, "Discrete Entropy and Relative Entropy Study on Nonlinear Clustering of Underwater and Arial Images", 2007 IEEE International Conference on Control Applications, pp.318-23, Oct 1-3, 2007, Singapore

[24] Z. Ye, H. Mohamadian and Y. Ye, "Information Measures for Biometric Identification via 2D Discrete Wavelet Transform", 2007 IEEE International Conference on Automation Science and Engineering, pp. 835-840, Sept. 22-25, 2007, Scottsdale, Arizona, USA

[25] Z. Ye, Y. Ye and H. Mohamadian, "Biometric Identification via PCA and ICA Based Pattern Recognition", 2007 IEEE International Conference on Control and Automation, pp. 1600-1604, May 30-June 1, 2007, Guangzhou, China

[26] Z. Ye, Y. Ye and H. Mohamadian, "Design of Fuzzy Stochastic Nearly Optimal Control", IEEE International Conference on Fuzzy Systems, pp. 8458-8462, July 16-21, 2006, Vancouver, Canada

[27] Z. Ye, J. Luo, P. Bhattacharya and Y. Ye, "Segmentation of Aerial Images and Satellite Images Using Unsupervised Nonlinear Approach", *WSEAS Transactions on Systems*, pp. 333-339, Issue 2, Volume 5, February, 2006